Pergamon

Ocean Engng, Vol. 22, No. 5, pp. 457–488, 1995
Elsevier Science Ltd
Printed in Great Britain
0029–8018/95 $9.50 + .00

0029–8018(94)00021-2

A TALE OF TWO WAVE TRAINS

Todd L. Walton Jr
U.S. Army Corps of Engineers, Coastal Engineering Research Center, U.S.A.E. Waterways Experiment Station, Vicksburg, MS, U.S.A.

(*Received for publication* 5 *August* 1994)

Abstract—The present study is an investigation into the transfer of the wave energy as it propagates through the surf zone and the consequent evolution of the wave trains and the corresponding envelope of the wave trains. The generation of long wave energy is investigated and one approach to developing the nonlinear transfer function for the transformation process is attempted. A nondimensionalized format for expressing the data is suggested for clarifying future studies of this type.

INTRODUCTION

The transfer of offshore measured wind wave spectra through the surf zone and up onto the beach to predict wave runup and overtopping is one of the remaining difficult coastal engineering problems to be solved. Numerous field and laboratory studies [i.e. Horikawa and Kuo (1966), Goda (1975), Battjes and Janssen (1978), Hotta and Mizuguchi (1980), Guza and Thornton (1982), Guza, Thornton and Holman (1984), Svendsen (1984), Holman and Sallenger (1985), Dally, Dean, and Dalrymple (1985) and Ebersole and Hughes (1987), to name but a few] have been made addressing the transfer of irregular waves and wave energy through the surf zone. These studies have addressed the difficulties inherent in such a transformation, that is, the nonlinear frequency shift of energy due to the wave breaking process and the unknown energy dissipation and transfer mechanisms acting within the surf zone.

The present study is a relook at a limited portion of an extensive laboratory data set [Smith and Vincent (1992)] in an attempt to clarify some of these energy transfer mechanisms. In addition, one particular system identification approach to studying the nonlinear transformation problem was attempted. Results of this unsuccessful approach are discussed along with suggestions for future ressearch. A new format for expressing the data is provided herein which if adapted should clarify future studies of this type.

DATA

The data utilized in the present approach was obtained in an extensive testing program of nearshore wave transformation by Smith and Vincent (1992). The testing was done in a Coastal Engineering Research Center wave flume at the U.S. Army Engineer Waterways Experiment Station. A number of cases of both single and double peaked spectra were selected for simulation in the testing program. Single peaked spectra were of the TMA form [Bouws *et al.* (1985)]. The shape of the double peaked spectra were determined by superimposing two spectra of TMA form. The wave flume

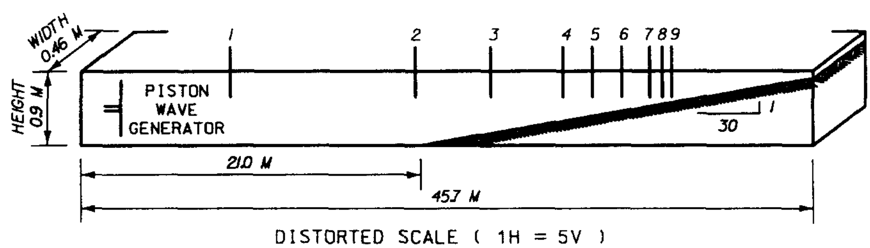

Fig. 1. Wave flume and gage locations.

utilized is as shown in Fig. 1 as adapted from Smith and Vincent (1992). The flume is 0.46 m wide, 45.7 m long, and 0.9 m deep. Irregular waves were generated on a horizontal bottom with a piston type wave paddle. At the approximate midpoint of the flume a transition from a horizontal bottom to a 1 in 30 slope begins. The flume bottom is smooth concrete and the side walls are of glass supported by steel beams. The water depth in the horizontal section of the flume was 61 cm. Nine electrical resistance gages were used to measure the variation of the free surface during the tests. The gages were in water depths of 61 cm, 61 cm, 46 cm, 30 cm, 24 cm, 18 cm, 12 cm, 9 cm and 6 cm. Gage locations are as shown in Fig. 1.

Data were sampled at 10 Hz for 1250 sec. The first 30 sec of data were not analyzed to ensure that the slower traveling high frequency components had reached the gage farthest from the paddle. Reflection coefficients based on past testing with similar wave period ranges and flume configuration were of the order of 5–10% [Smith and Vincent (1992)]. Extensive discussion of this set of tests as well as of wave transformation is given in Smith and Vincent (1992).

The present analysis was conducted on a subset of the Smith and Vincent (1992) data set. Two spectra were chosen that were of similar energy content overall but consisted of one peak in case one (referred to as "wt1" for wave train 1) and two peaks having approximately 50% of the energy each in case two (referred to as "wt2" for wave train 2). The breakdown of the peak periods T_p and energy content H_{mo} for the two wave trains is provided in Table 1. Additional details of the analysis are discussed in Walton (1991).

ANALYSIS

The first set of plots consists of various stages of the wave transformation as the wave train moves across the 1 in 30 slope into the progressively shallower water. Figure 2(a)–(c) shows the wt1 wave train surface elevation at the offshore gage (and its envelope amplitude spectra as a dashed line), the wave train surface elevation spectra

Table 1. Characteristics of single and double peaked wave train

Type	$T_p^{(1)}$ (sec)	$H_{mo}^{(1)}$ (cm)	$T_p^{(2)}$ (sec)	$H_{mo}^{(2)}$ (cm)	$H_{mo}^{(\mathrm{total})}$ (cm)
Single peak	2.5	15.2	–	–	15.2
Double peak	2.5	6.5	1.75	6.5	9.1

(and the envelope amplitude spectra as a dashed line), and the cumulative energy distribution as a function of frequency for the surface elevation (and for the envelope amplitude as a dashed line) respectively. Spectral plots were averaged for 32 degrees of freedom and normalized by the variance of the water level signal at each depth. Linear scales have been utilized for ease of interpretation and insight into engineering significance of the energy changes within given frequency bands. As would be expected of a random narrow banded Gaussian process, the envelope amplitude has its energy at considerably lower frequencies than the wave train itself. In the present example wave amplitude time series $A(t)$ can be found via wave envelope analysis utilizing Hilbert transform techniques. Assuming that sea surface elevation $\eta(t)$ is a realization of an ergodic Gaussian process, it can be defined in the following manner:

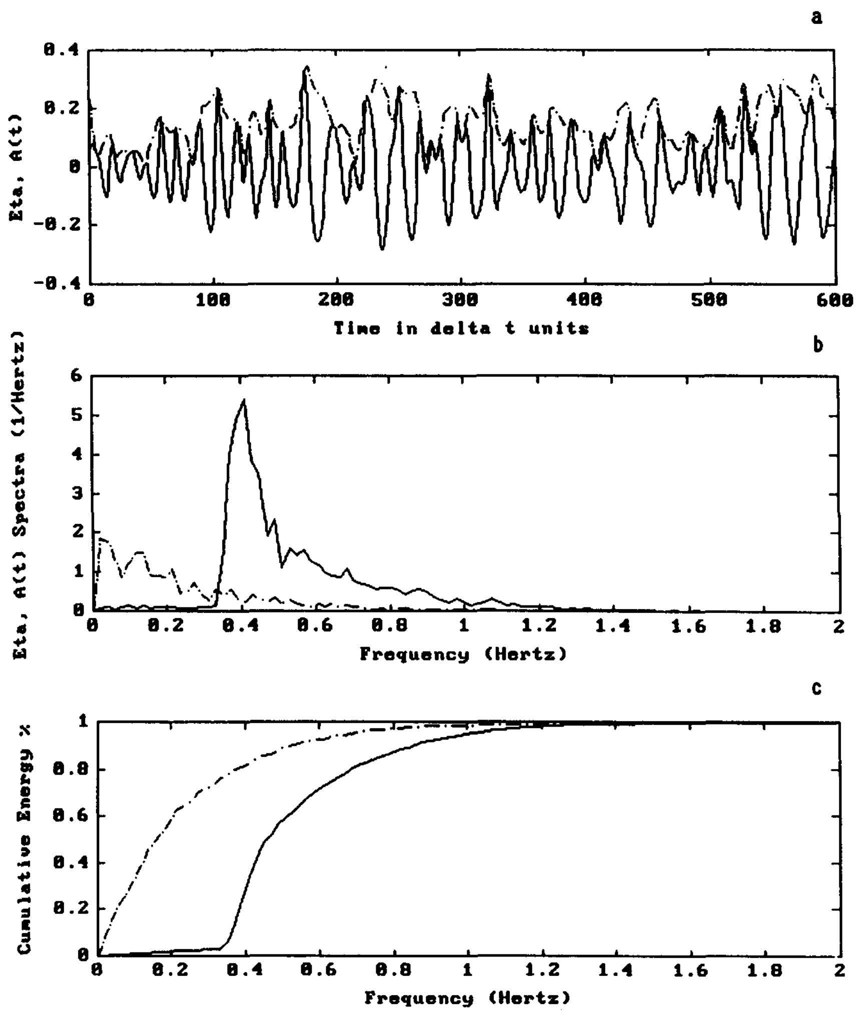

Fig. 2. (a) Time series, (b) spectra, and (c) cumulative energy wt1.

$$\eta(t) = \sum_{m=1}^{N} A_m \cos(2\pi f_m t + \theta_m) \ , \tag{1}$$

where N = number of discrete Fourier components (amplitudes), A_m = amplitude of mth component, f_m = frequency of mth component and θ_m = phase of mth component (assumed random and uniformly distributed over a 2π interval). Bendat and Piersol (1986) define the Hilbert transform of $\eta(t)$ as follows:

$$\hat{\eta}(t) = \sum_{m=1}^{N} A_m \sin(2\pi f_m t + \theta_m) \ , \tag{2}$$

which is basically Equation 1 shifted by $\frac{\pi}{2}$. They also define the analytic signal as:

$$z(t) = \eta(t) + \mathrm{j}\hat{\eta}(t) = A(t) \exp \mathrm{j}(\theta(t) + \phi) \ , \tag{3}$$

where $\mathrm{j} = \sqrt{-1}$, $A(t)$ = amplitude of the envelope, and $\theta(t) + \phi$ = phase angle. The instantaneous function of wave amplitude $A(t)$ is then defined as follows:

$$A(t) = \sqrt{\eta^2(t) + \hat{\eta}^2(t)} \ . \tag{4}$$

To calculate the instantaneous function of wave amplitude using Equation 4 requires the Hilbert transform of $\eta(t)$ from Equation 2. The most efficient means of calculating the Hilbert transform is via the frequency domain method as discussed in Bendat and Piersol (1986). This approach was utilized in the present procedures. Figures 2–10 are for wt1 as measured at gages 1–9 in water depths of 61 cm, 61 cm, 46 cm, 30 cm, 24 cm, 18 cm, 12 cm, 9 cm and 6 cm respectively. Similar plots are also provided for wt2 in Figs 11–19 for the same set of wave gage measurement locations.

General observations of the transformation plots point out the following items for both the single and double peaked spectra: (1) the nondimensionalized energy spreads in both a low and high frequency direction from the original band limited offshore signal although the predominant preferential shift of energy is to the lower frequencies, (2) the envelope amplitude calculated spectrum evolves to a shape similar to the water surface elevation spectrum and (3) the envelope amplitude cumulative energy distribution with frequency evolves to a shape similar to the water surface elevation cumulative energy distribution with frequency. These observations all signify a breakdown of the group structure through the surf zone. It should be noted that in the above analysis the wave train has been treated as a system of progressive waves in form; separation of incident and reflected wave parameters is not made. This analysis is reasonably consistent with comments of Smith and Vincent (1992) that reflection was very low, 5–10%, and with observations on natural beaches [Walton (1992)]. Additional plots of the dimensionalized spectra (not shown) suggest a minor portion of energy is shifted to low frequencies (including the mean setup) while the majority of the frequencies lose energy in the dissipation process (which is partially converted into the low frequency portion of the water surface elevation).

A second type of plot is shown in Fig. 20 where Fig. 20(a) is the Fourier component amplitude of the wt1 offshore wave train while Fig. 20(b) is the Fourier component phase (in radians) of the same wave train, both presented as a function of "dimensionless" frequency. Both amplitude and phase were averaged over 16 frequency bands for 32 degrees of freedom. It is a common assumption that in deeper water the wave

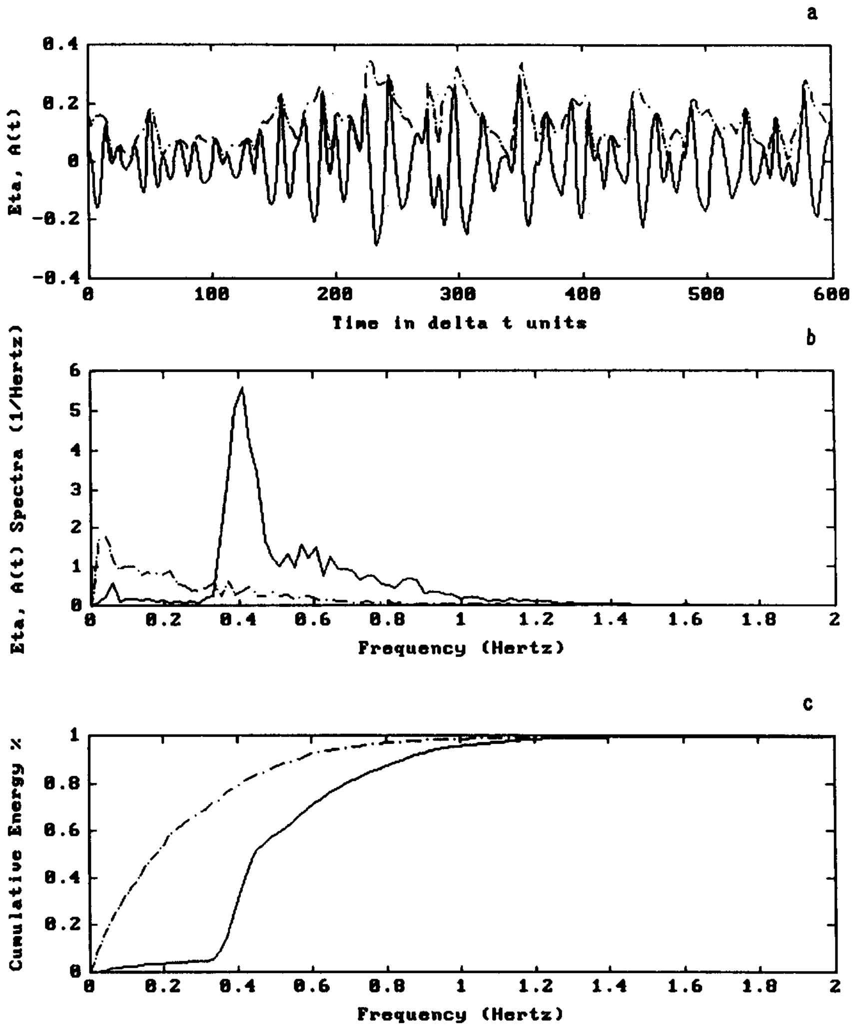

Fig. 3. (a) Time series, (b) spectra, and (c) cumulative energy wt1.

train consists of a summation of harmonic waves with Rayleigh distributed amplitude and random phasing assumed uniform over an interval $[0, 2\pi]$. This phenomena appears to be a reasonable assumption in deeper water as determined in field measurements [Rye (1982), Elgar *et al.* (1984, 1985)]. In the present situation, laboratory waves are generated in accordance with these assumptions hence the phasing in the offshore gage is in fact random. In the phase plots provided here the "unwrapped" phase is given as per Tribolet (1977). The "wrapped" phase (i.e. phase modulo 2π) would appear more random in a simple plotting due to limited vertical scale interval $[-\pi,\pi]$.

Figs 20–25 are for wt1 proceeding from offshore to inshore in depths of water equal to 61 cm, 61 cm, 46 cm, 30 cm, 24 cm, 18 cm, 12 cm, 9 cm and 6 cm respectively.

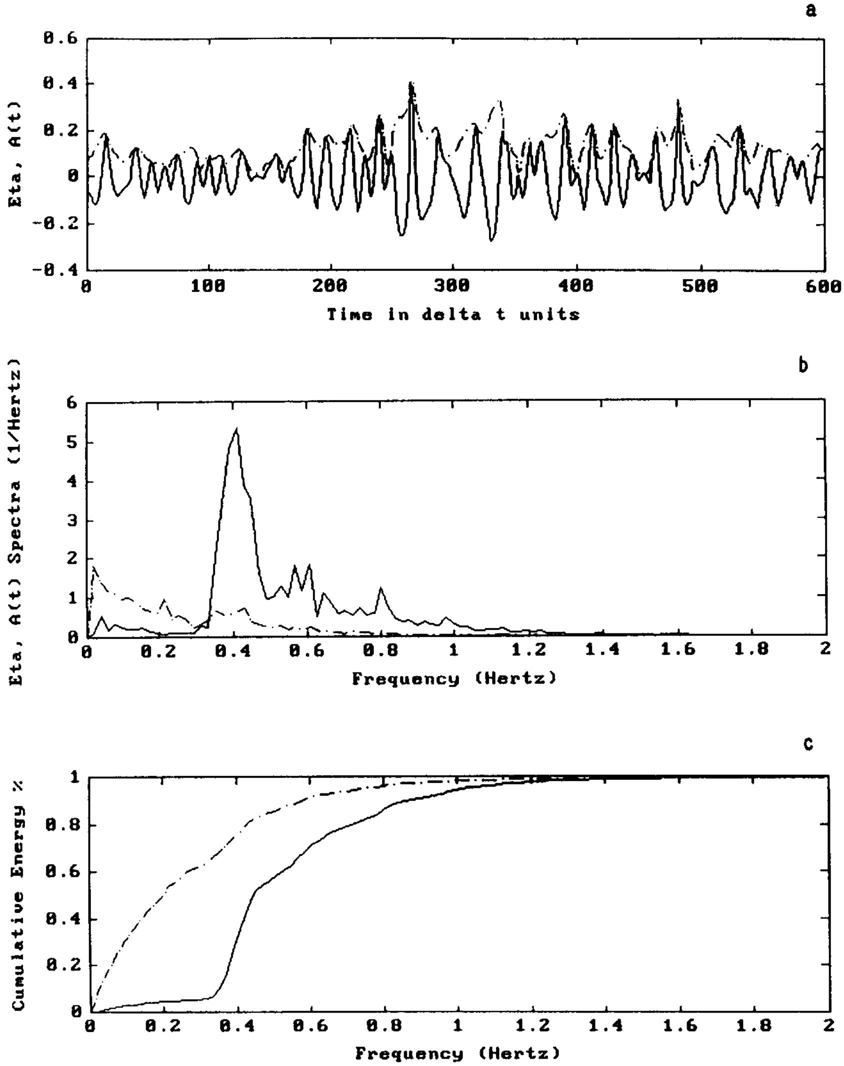

Fig. 4. (a) Time series, (b) spectra, and (c) cumulative energy wt1.

Figures 26–30 are similar plots for wt2 in the same water depths (except 0.09 m depth omitted). The horizontal scale in these plots is a nondimensional frequency $\left(\hat{f} = f\sqrt{\frac{2\pi d}{g}}\right)$ that allows determination as to whether the given frequency component is in "shallow" water $\left(\frac{d}{L_o} \leq 0.02 \text{ or } \hat{f} \leq 0.14\right)$ according to linear wave theory where waves would be nondispersive as opposed to "transitional" or "deep" water where the waves would still be dispersive in frequency. It might be expected that in the lower nondimensionalized frequencies (i.e. shallow water), the wave phasing might be less

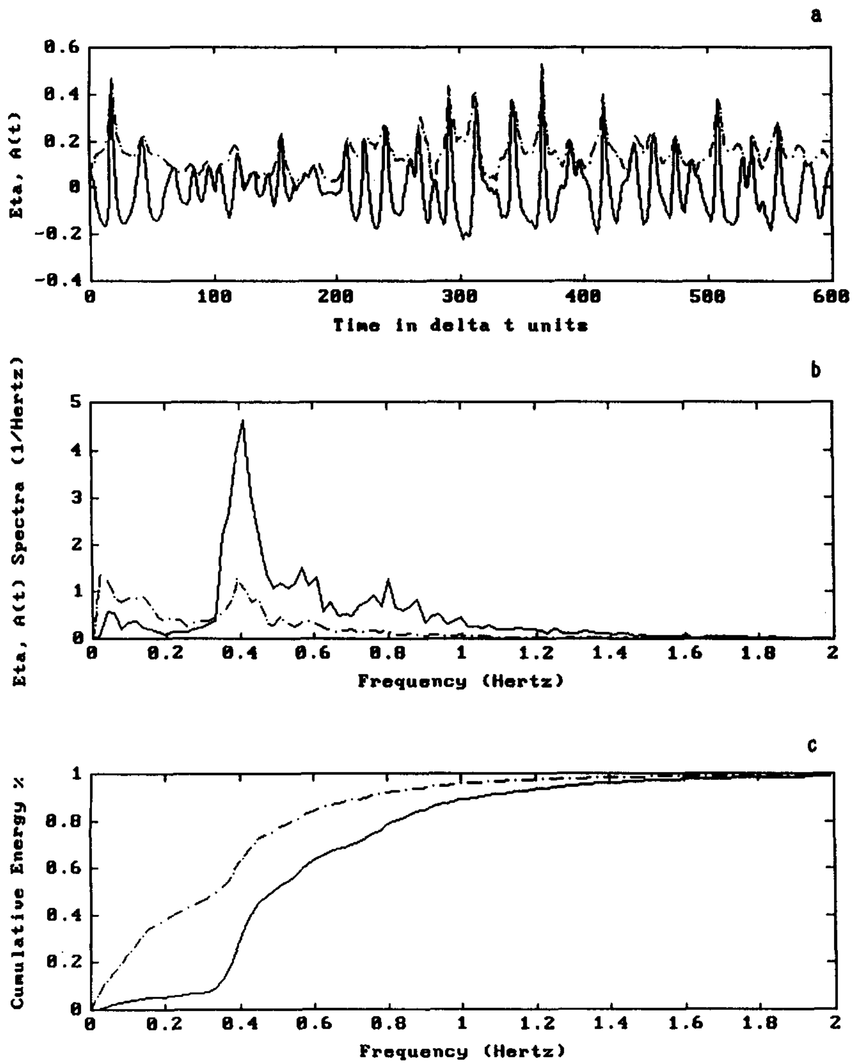

Fig. 5. (a) Time series, (b) spectra, and (c) cumulative energy wt1.

random and hence more order might be apparent in the unwrapped phase due to the nature of nondispersive waves. A study of numerous realizations of the wave train using this type of plot might provide insight into the dual random/deterministic aspects of wave transformation through the surf zone.

It is apparent that there is nonlinearity in the (surf zone) system as can be seen via the time series itself and via probability distribution plots. Figures 31 and 32 show both the time series and the probability distribution as measured for the offshore gage and the most inshore gage for wt2. The solid line on the probability density function plots is of a fitted Gaussian distribution in which the mean and standard deviation

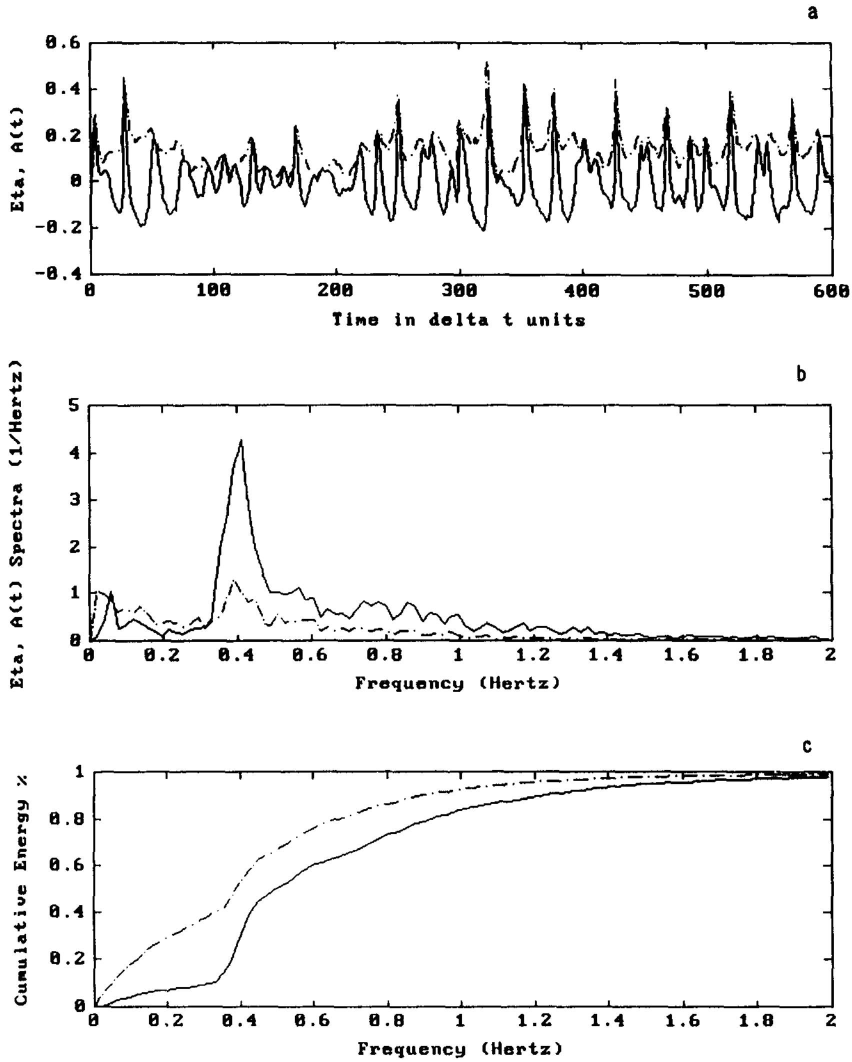

Fig. 6. (a) Time series, (b) spectra, and (c) cumulative energy wt1.

have been calculated from the data itself. As can be seen from these plots the offshore series complies with the Gaussian distribution assumption while the inshore series for wt2 is non-Gaussian. Similar results were found for wt1. As one of the characteristics of a linear system provides that Gaussian input produces Gaussian output, it is clear that the system does in fact have nonlinearity in it and must be treated (at least in an input/output systems approach) as a nonlinear system. The following section discusses one approach that was attempted (unsuccessfully) to address this nonlinearity.

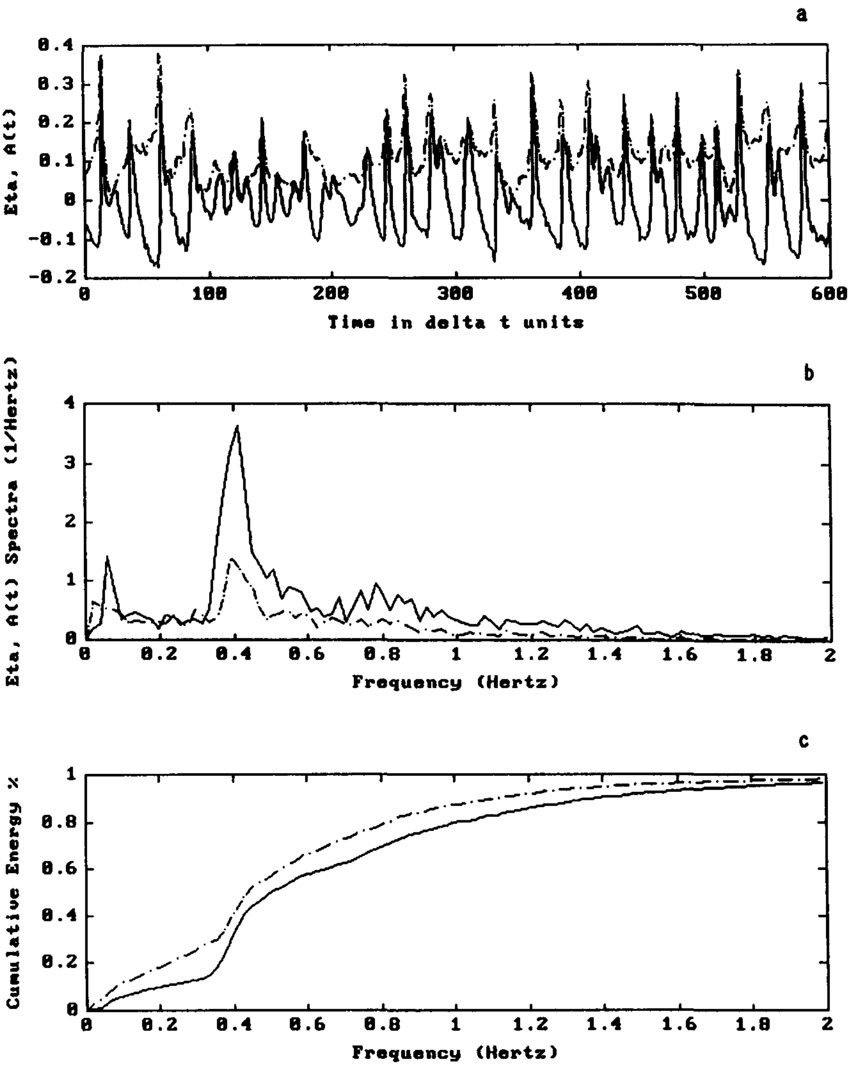

Fig. 7. (a) Time series, (b) spectra, and (c) cumulative energy wt1.

SYSTEM IDENTIFICATION APPROACH

One approach that has been utilized to handle weakly nonlinear system single input–single output problems is via zero-memory square and cubic law systems followed by linear filters in a transformed multiple input–single output system [Bendat (1990)]. In this case of correlated input the transformed input signal(s) which would consist of the squares and cubes of the original single system input signal must be conditioned to remove the linear effects of preceeding transformed input signals from succeeding transformed input signals (i.e. square of original input signal must remove the portion of the linearly related input signal prior to its use as input) as per Bendat and Piersol (1986). The use of a system approach such as discussed in Bendat (1990) is a simple

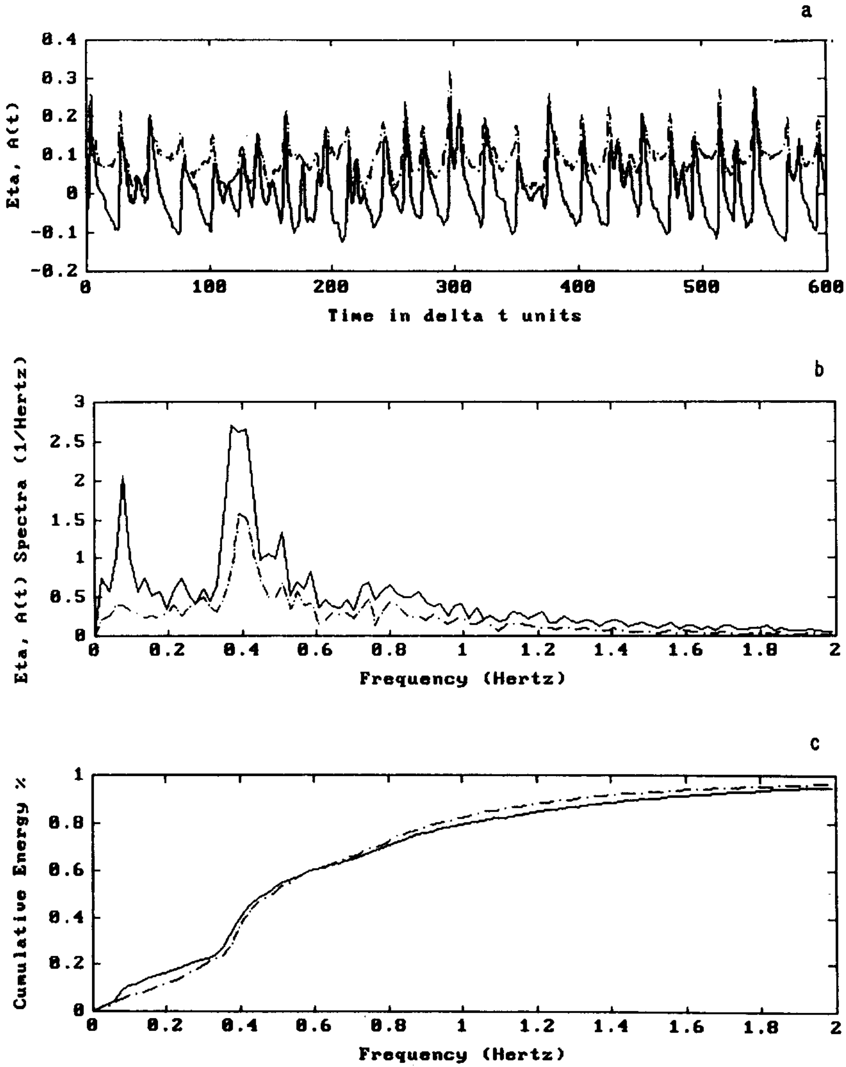

Fig. 8. (a) Time series, (b) spectra, and (c) cumulative energy wt1.

approach that does not require computation of the bispectral or trispectral density functions and can apply to non-Gaussian data as well as Gaussian data. These techniques have been employed successfully to handle weakly nonlinear problems in wave forces [Bendat and Piersol (1986)] and nonlinear drift forces on vessels [Bendat (1990)].

In the present case the input data from the offshore gage is Gaussian which simplifies the required system identification process since conditioning of inputs is not required in this situation. A specific problem not discussed in Bendat (1990) that must be dealt with in the present analysis is the time delay between input and output. An idealized approach to this problem is to develop a time delay for each frequency bandwidth

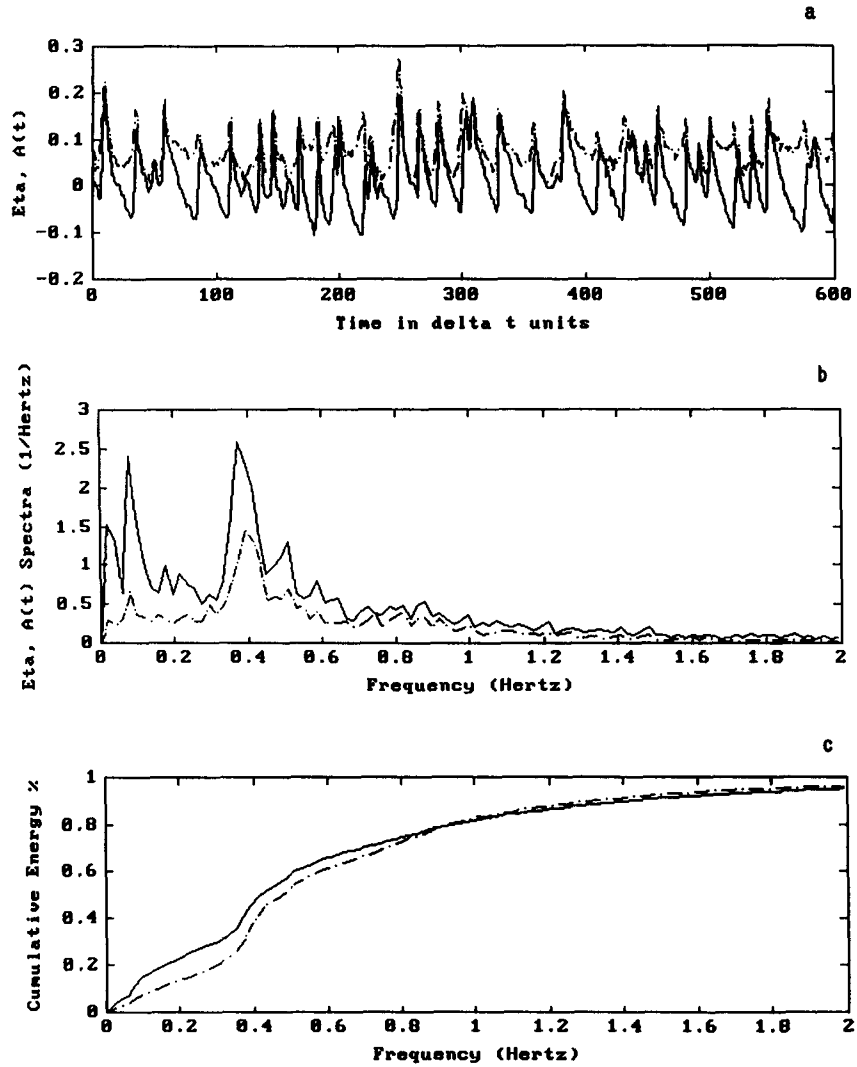

Fig. 9. (a) Time series, (b) spectra, and (c) cumulative energy wt1.

(due to the dispersive nature of water waves over the sloping bottom), then realign (in time) the series bandwidth by bandwidth prior to the system identification discussed below. In the present case the time delays over the frequencies of interest were not widely variable due to the nondispersive characteristics of shallow water waves; hence, the series inputs were time aligned by an average delay factor.

Two system identification techniques were utilized to determine the potential of the methodology. The first system utilized was a parallel system of input, squared input, and cubed input as per fig. 5.3 in Bendat (1990). Resulting system identification can be checked via the linear and nonlinear coherence functions as defined via equations

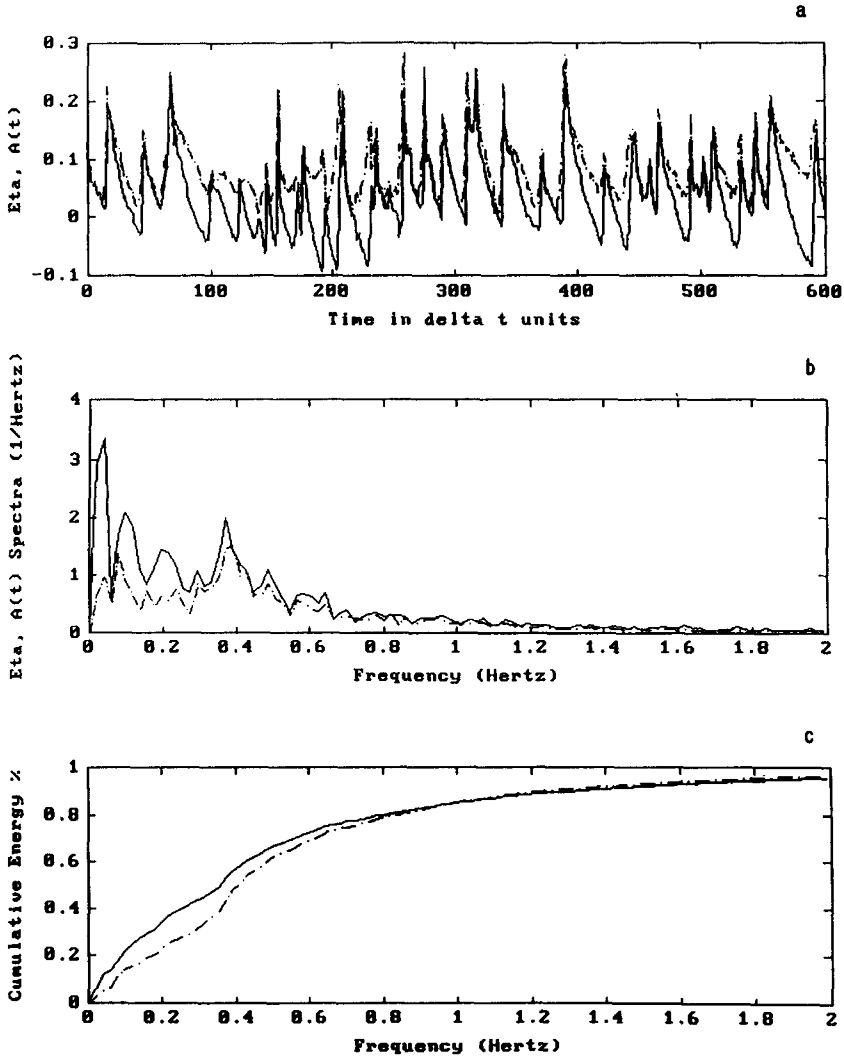

Fig. 10. (a) Time series, (b) spectra, and (c) cumulative energy wt1.

5.29–5.31 in Bendat (1990). The input and output wave trains and their respective nondimensionalized spectra for wt2 were shown earlier in Figs 11 and 19. Figure 33(a) shows the standard linear coherence squared of the input (offshore) and output (inshore) signals for wt2 again showing that the system is in fact nonlinear. The present total coherence of the revised multiple input–single output nonlinear system approach 1 discussed above is shown in Fig. 33(b). As seen in this figure, the lack of high coherence in this system suggests that low order polynomial modeling is not promising in a strongly nonlinear system of this type. Similar results were found for the same analysis of wt1.

The second system utilized is as shown in fig 7.15 of Bendat (1990) where the input

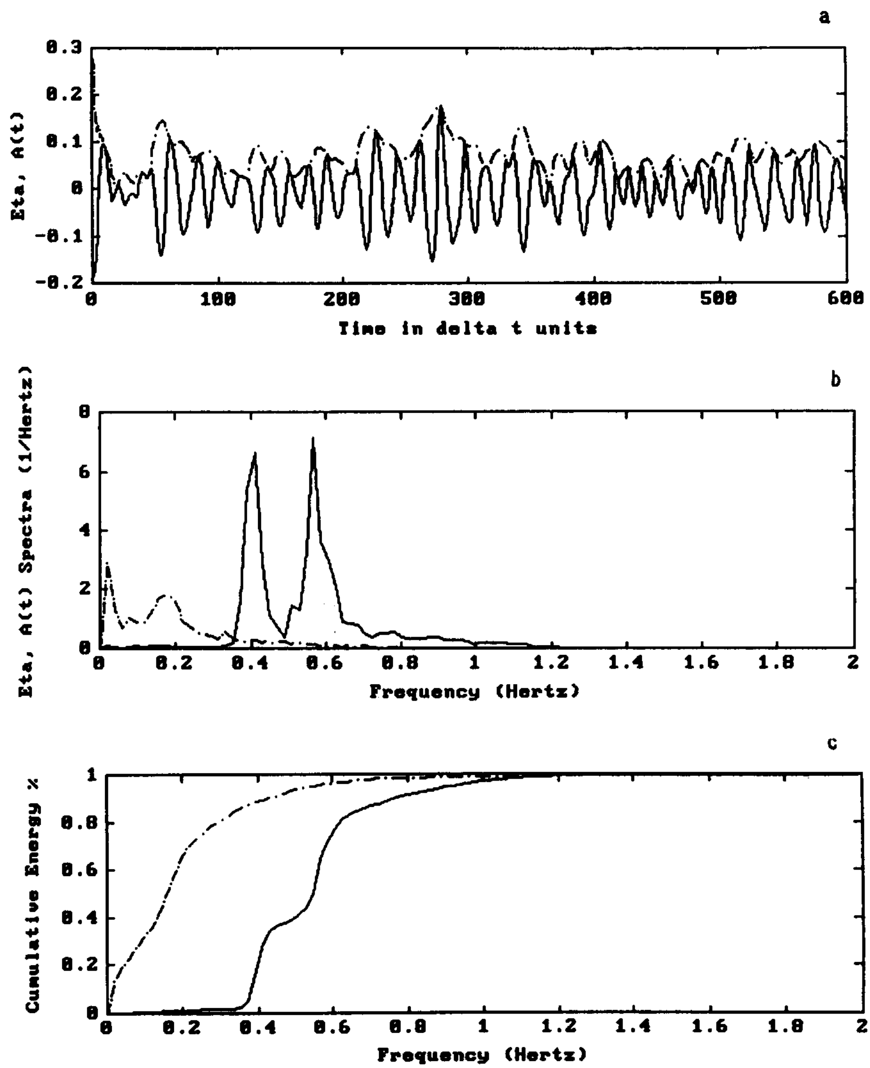

Fig. 11. (a) Time series, (b) spectra, and (c) cumulative energy wt2.

signals consist of the water surface elevation and the envelope amplitude function of the offshore gage. The system itself is described via equations 7.121–7.123 in Bendat (1990) while the linear and nonlinear coherence functions are given in equations 7.115 and 7.116 of the same reference. The total coherence of this particular system is shown in Fig. 34 for wt2 with 32 degrees of freedom. Again total coherence is low and results of this system identification approach are not promising for the strongly nonlinear system of the type given here. Similar results were found for the same analysis of wt1.

Energy dissipation and wave setup characteristics of the two wave trains as well as modification of their envelope characteristics are shown in Figs 35–38.

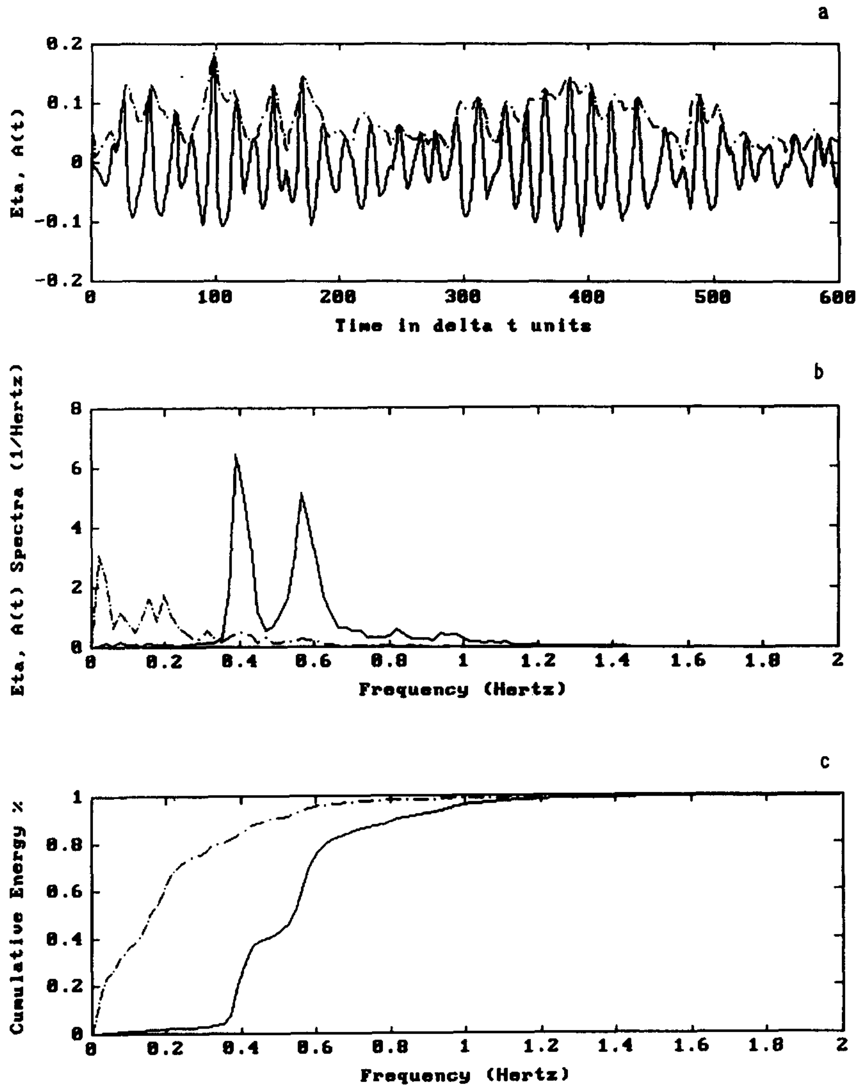

Fig. 12. (a) Time series, (b) spectra, and (c) cumulative energy wt2.

CONCLUSIONS

A small segment of data from a large database of nearshore wave transformation data was evaluated in depth to provide a better understanding of nearshore wave transformation. Certain properties of the transformation process provide potential avenues for further research. One such area where further research is needed is on the transformation of the wave spectra or equivalent envelope amplitude function through the nearshore. Ability to better define the nearshore transformation of waves may profit from an ability to predict the envelope amplitude function which should be more clearly governed by the nearshore bottom slope and depth at the given location

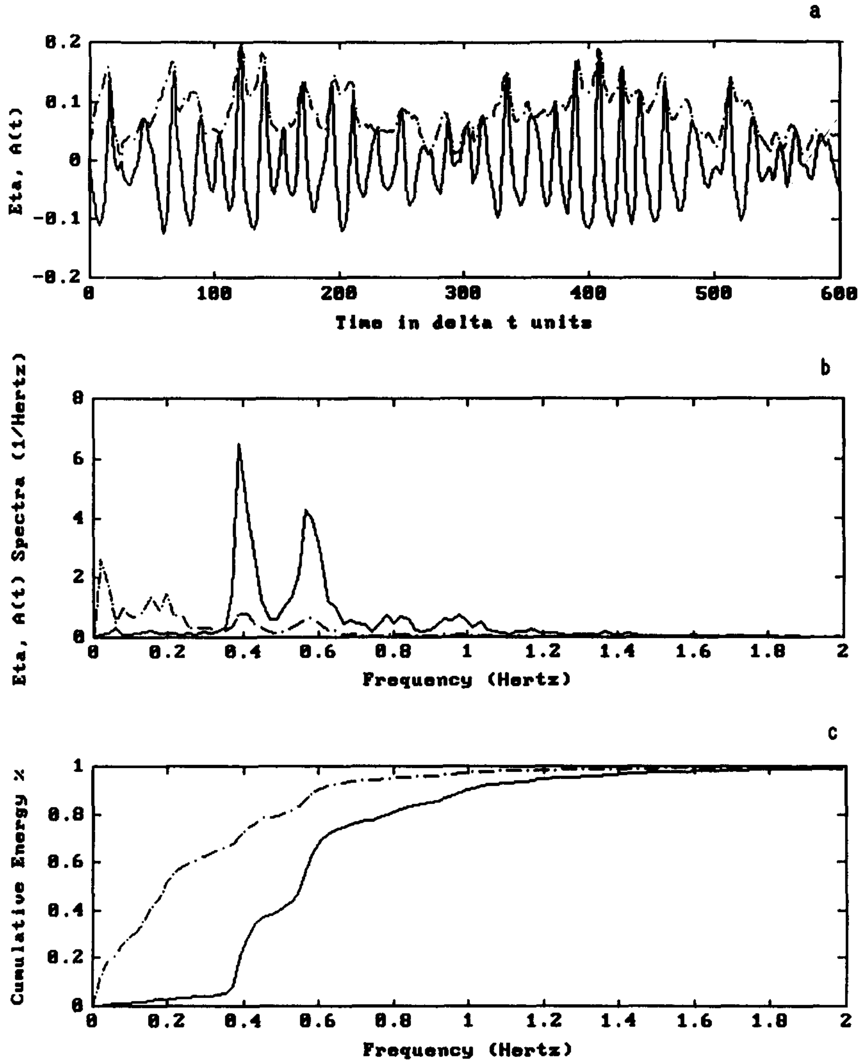

Fig. 13. (a) Time series, (b) spectra, and (c) cumulative energy wt2.

where prediction is desired. Additionally, ability to predict the changing unwrapped phase through the surf zone may also be important in predicting wave transformation and lead ultimately to a better understanding of wave runup. A proposed nondimensional frequency axis for phase plots which defines the "shallowness" at the site for various frequency bands may be a key to improved understanding of the transformation process.

Two simplified system identification techniques were attempted without much success for the data sets investigated. The failure of such approaches to provide high total coherence appears due to the strong nonlinearity induced by the apparent chaotic

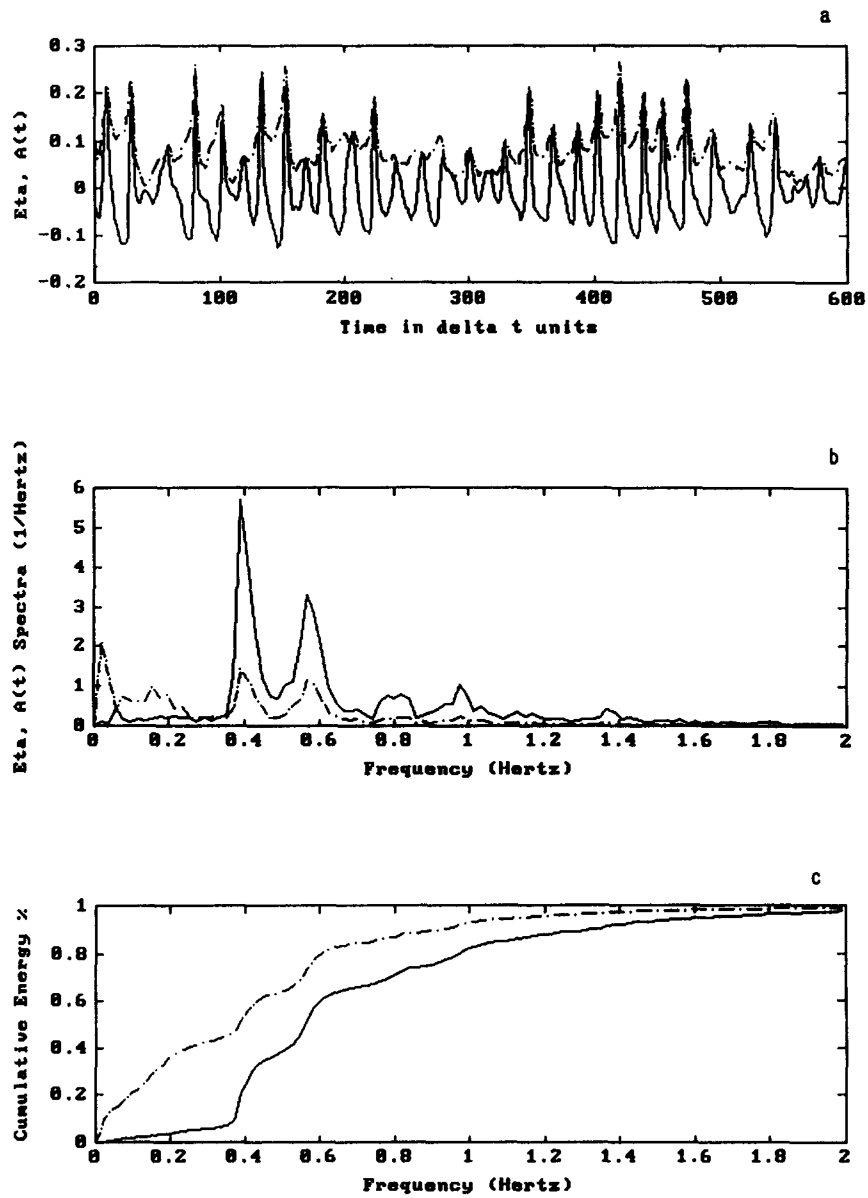

Fig. 14. (a) Time series, (b) spectra, and (c) cumulative energy wt2.

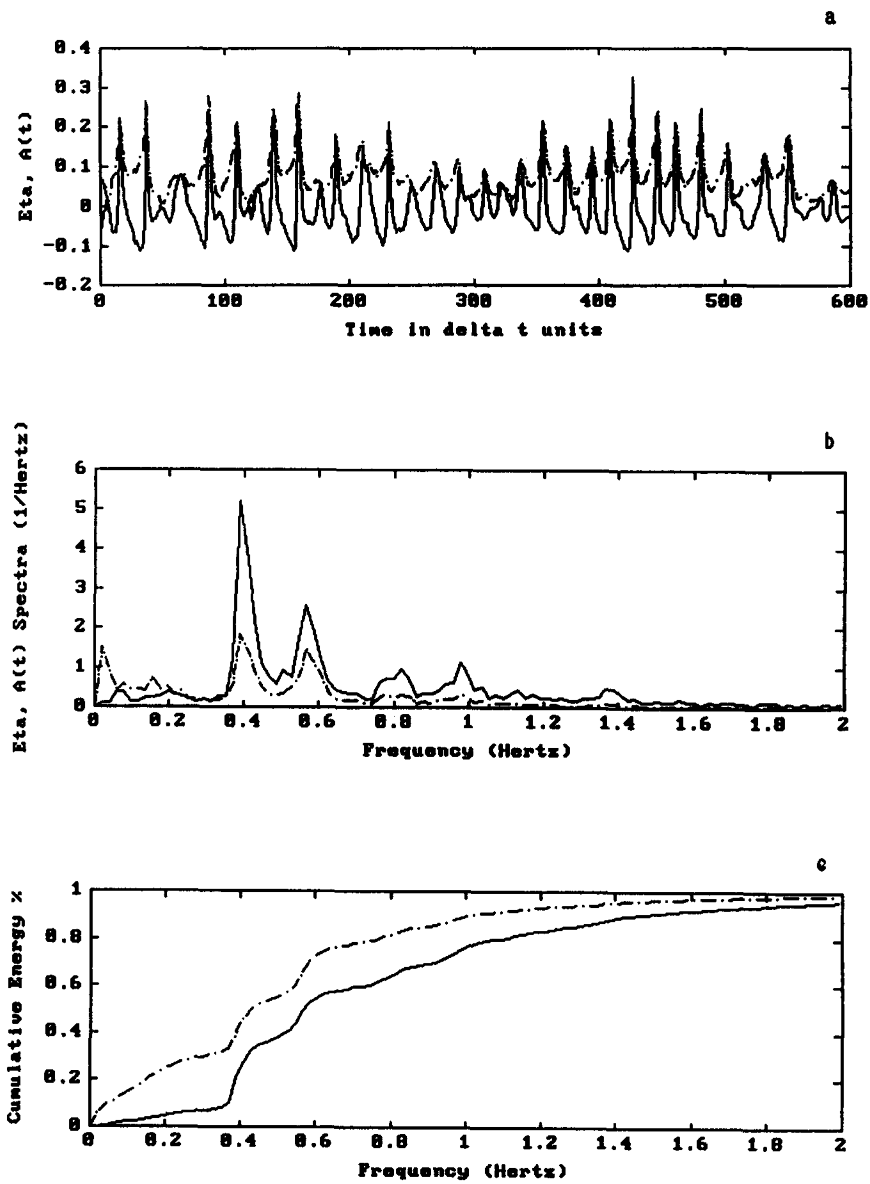

Fig. 15. (a) Time series, (b) spectra, and (c) cumulative energy wt2.

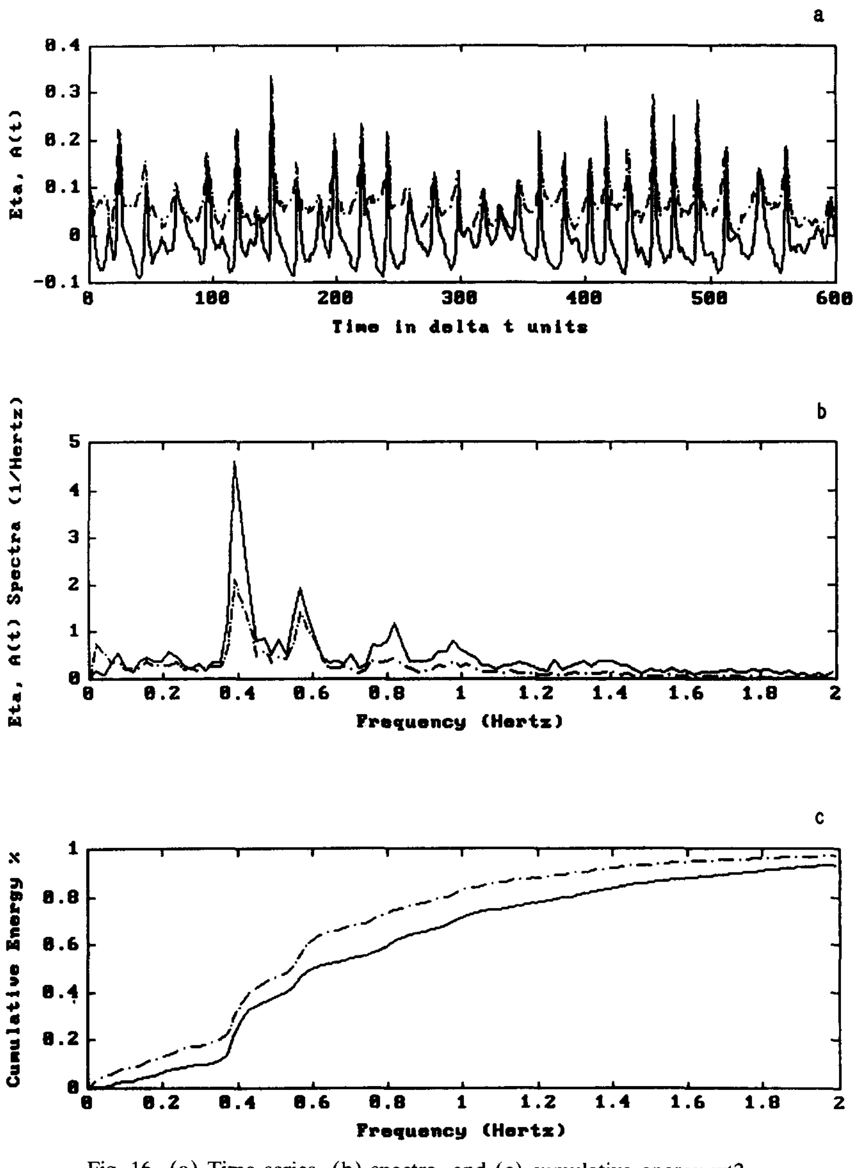

Fig. 16. (a) Time series, (b) spectra, and (c) cumulative energy wt2.

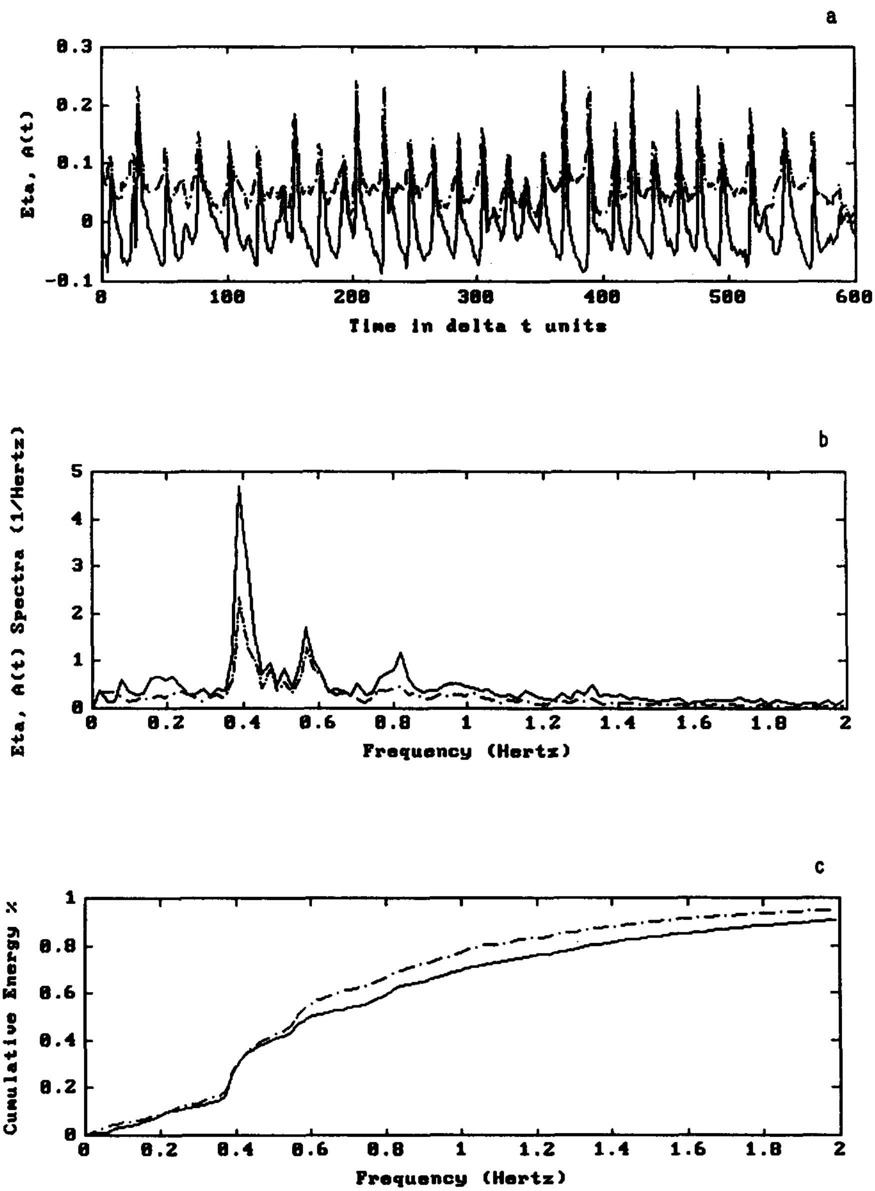

Fig. 17. (a) Time series, (b) spectra, and (c) cumulative energy wt2.

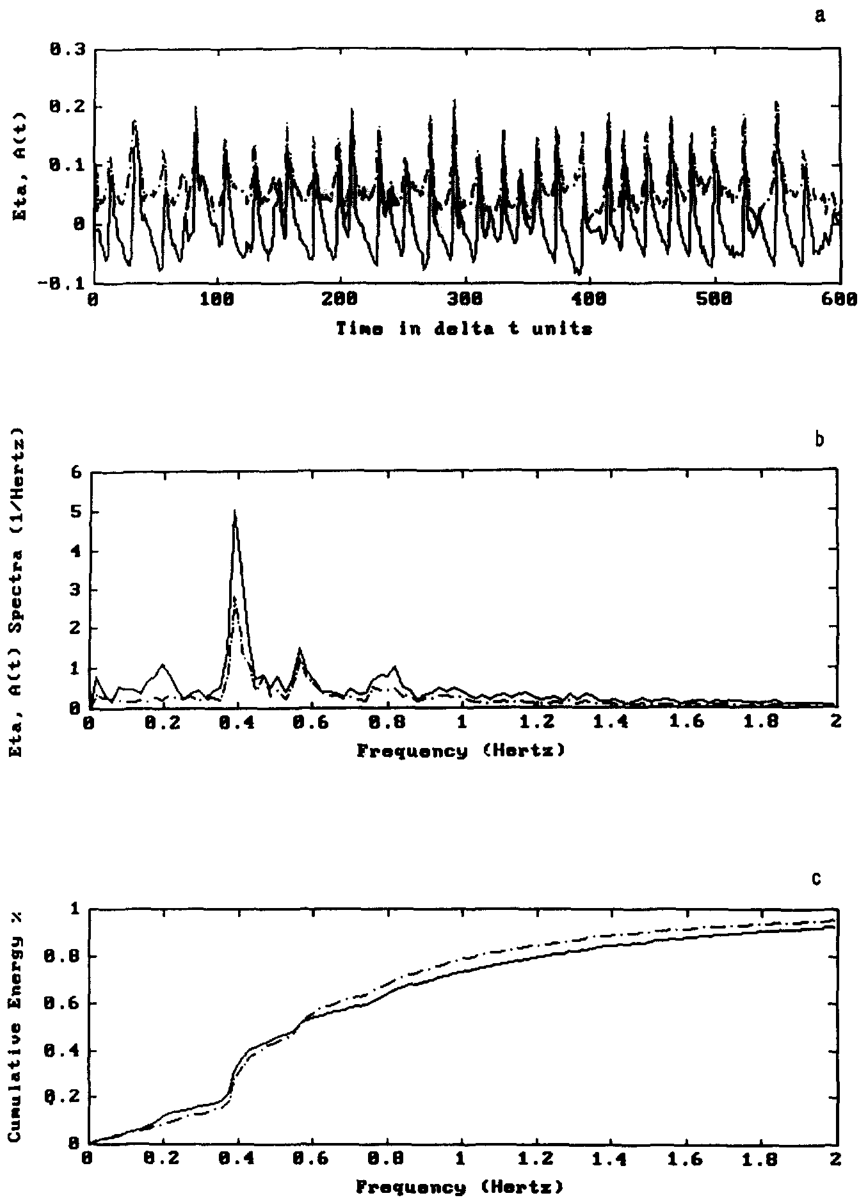

Fig. 18. (a) Time series, (b) spectra, and (c) cumulative energy wt2.

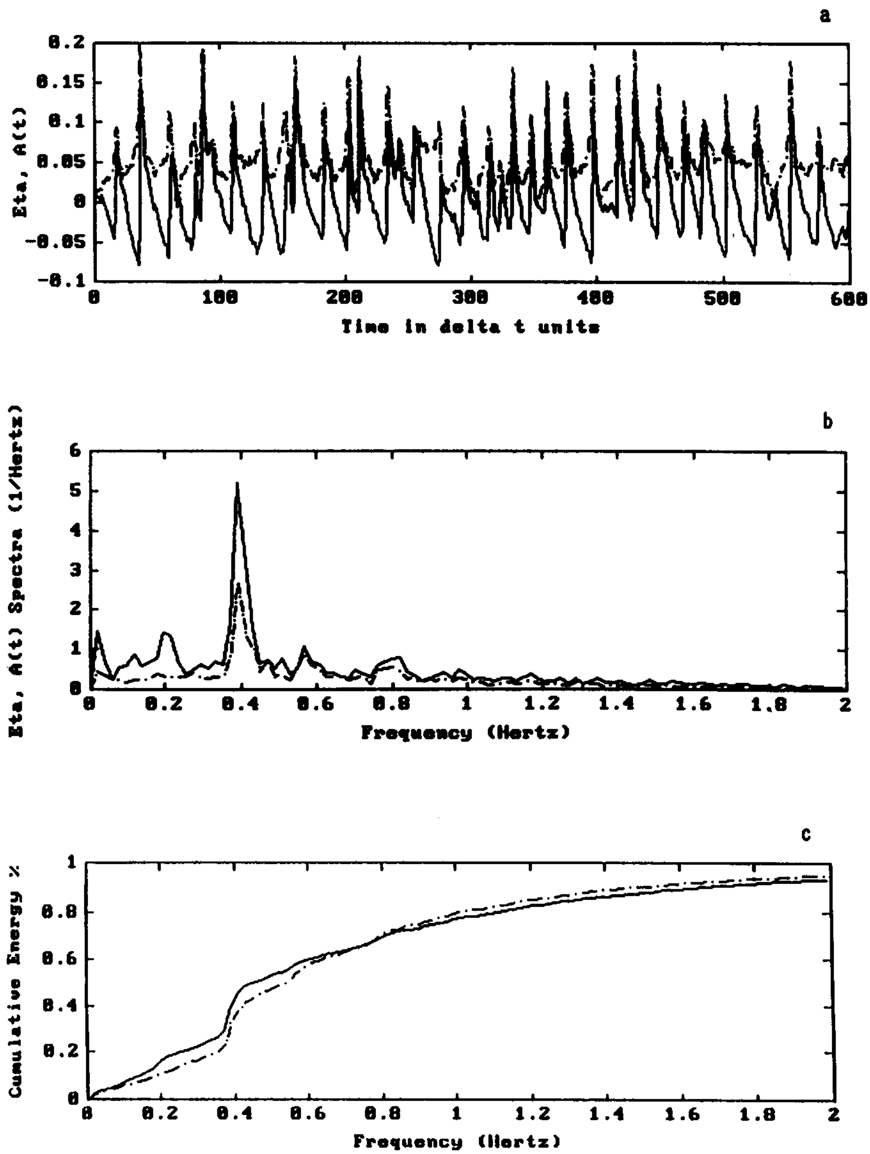

Fig. 19. (a) Time series, (b) spectra, and (c) cumulative energy wt2.

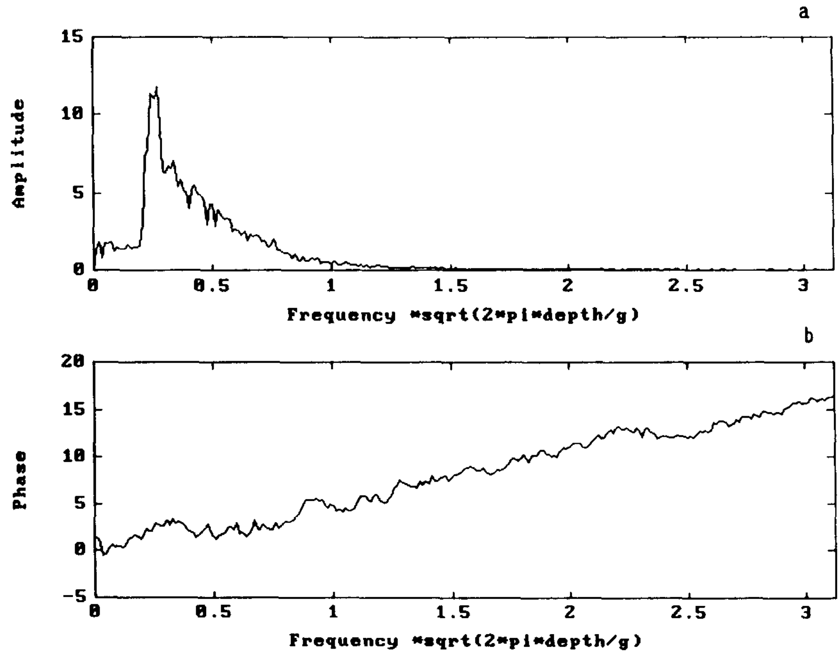

Fig. 20. Frequency component, (a) magnitude, and (b) phase wt1.

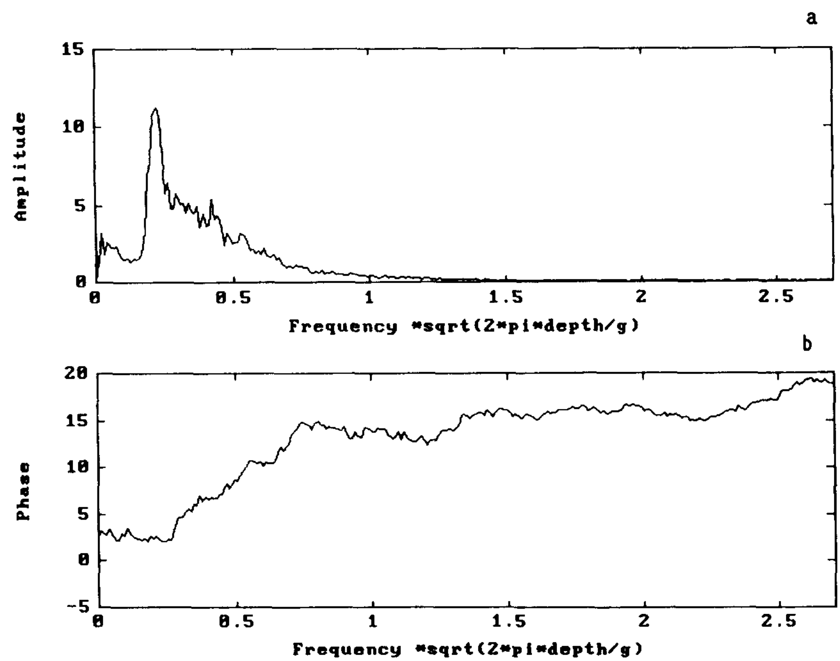

Fig. 21. Frequency component, (a) magnitude, and (b) phase wt1.

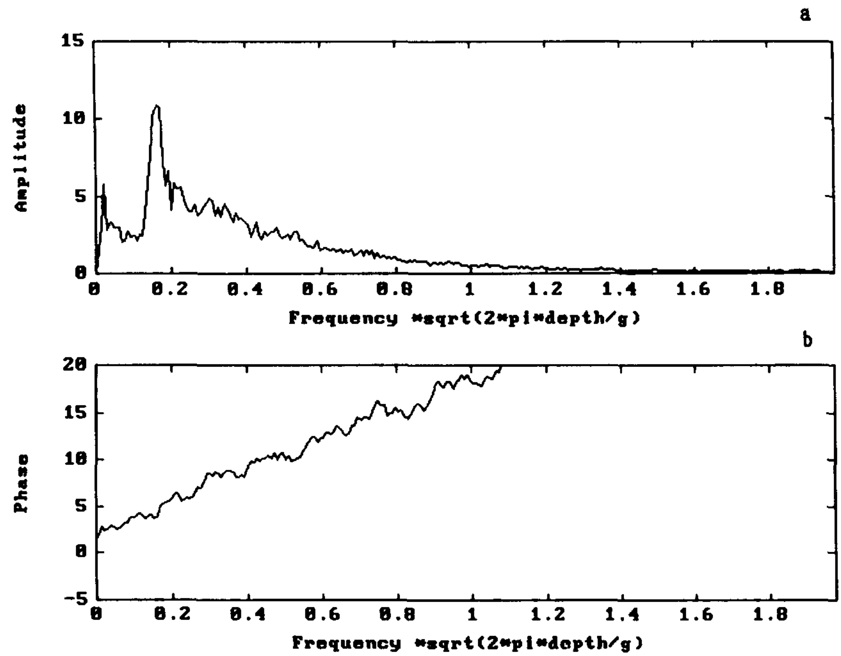

Fig. 22. Frequency component, (a) magnitude, and (b) phase wt1.

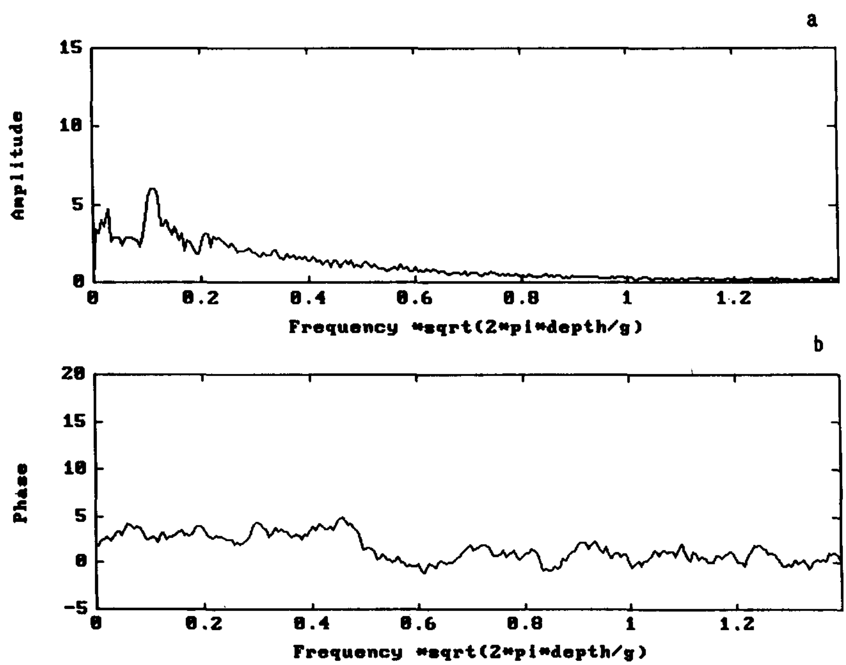

Fig. 23. Frequency component, (a) magnitude, and (b) phase wt1.

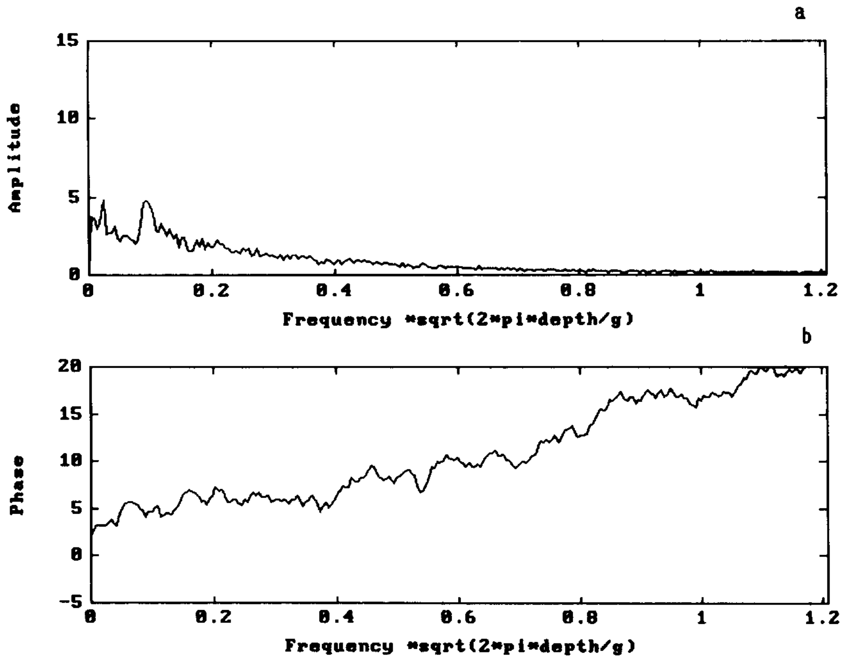

Fig. 24. Frequency component, (a) magnitude, and (b) phase wt1.

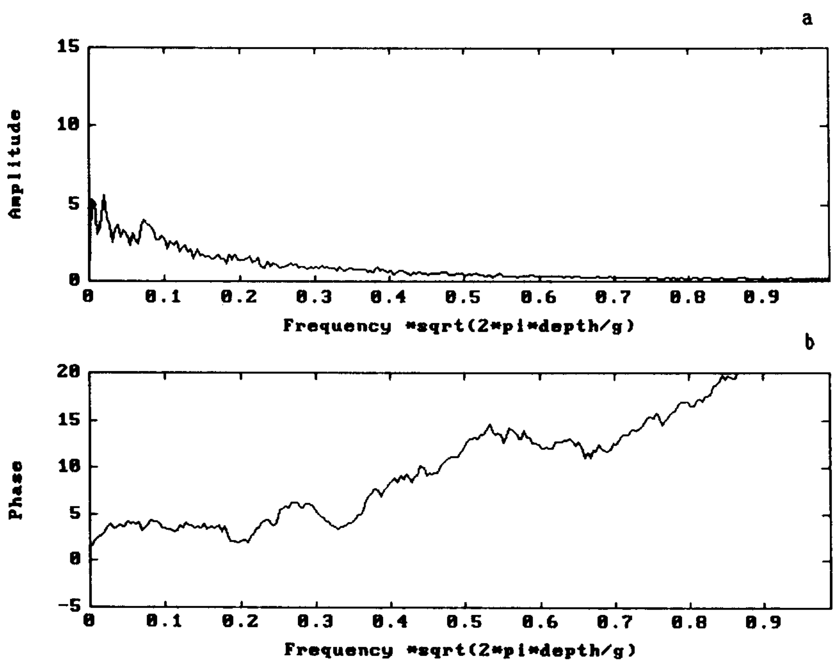

Fig. 25. Frequency component, (a) magnitude, and (b) phase wt1.

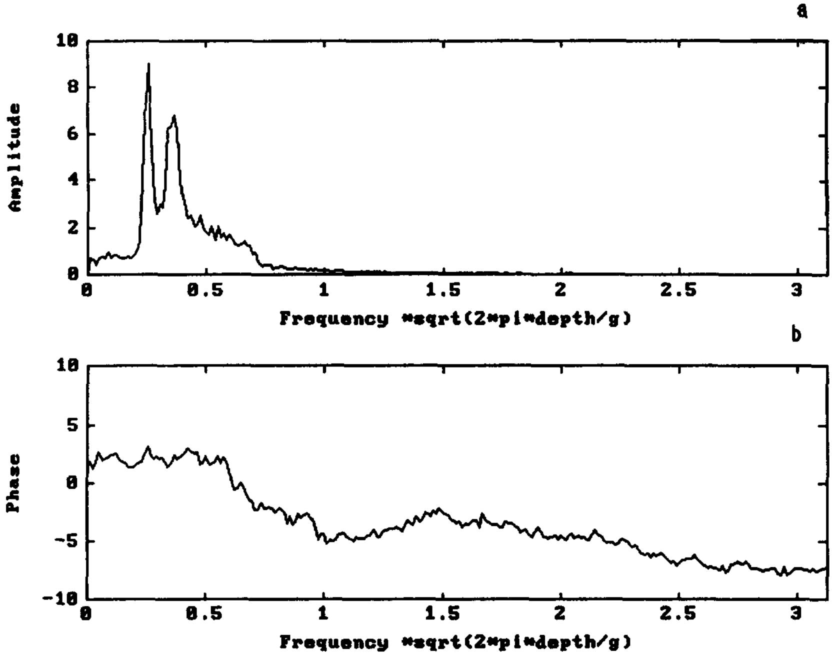

Fig. 26. Frequency component, (a) magnitude, and (b) phase wt2.

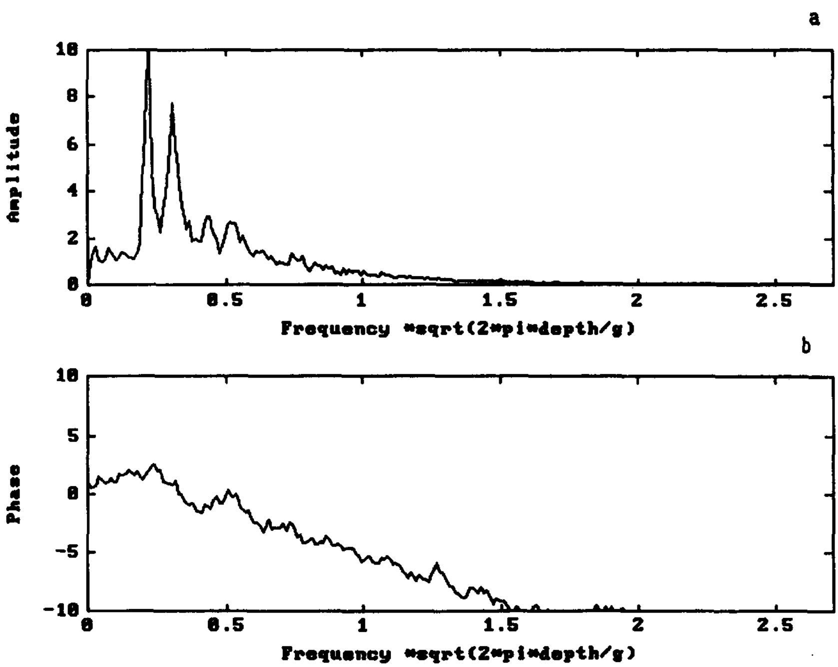

Fig. 27. Frequency component, (a) magnitude, and (b) phase wt2.

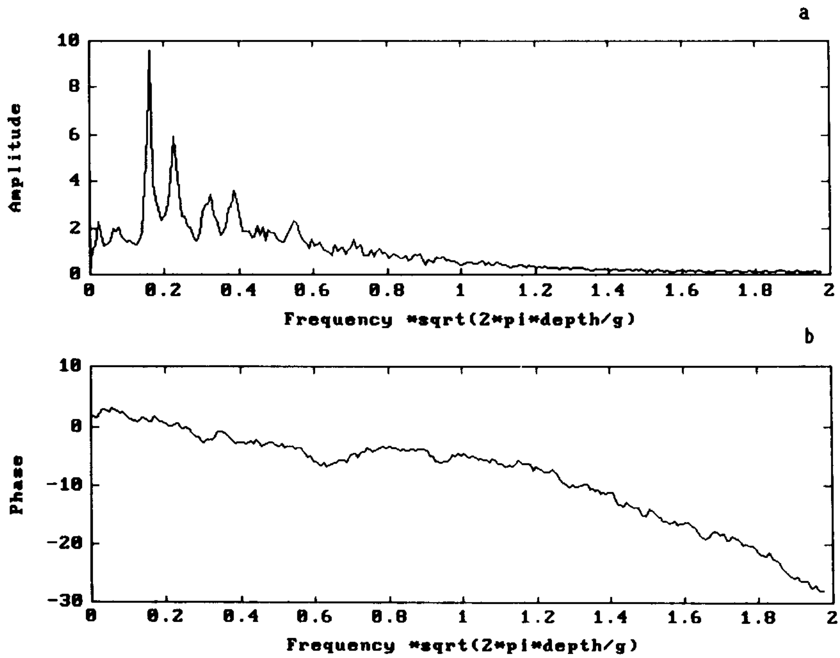

Fig. 28. Frequency component, (a) magnitude, and (b) phase wt2.

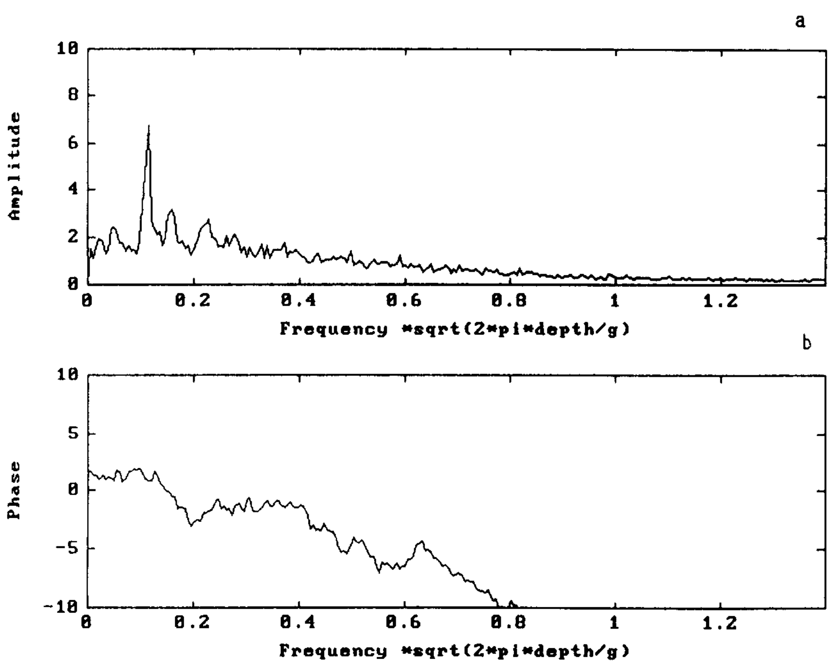

Fig. 29. Frequency component, (a) magnitude, and (b) phase wt2.

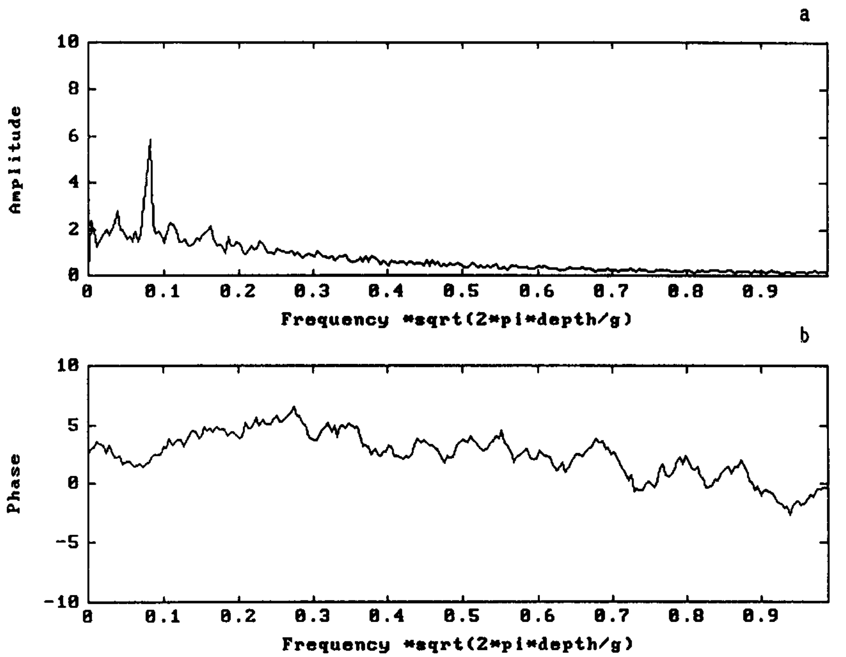

Fig. 30. Frequency component, (a) magnitude, and (b) phase wt2.

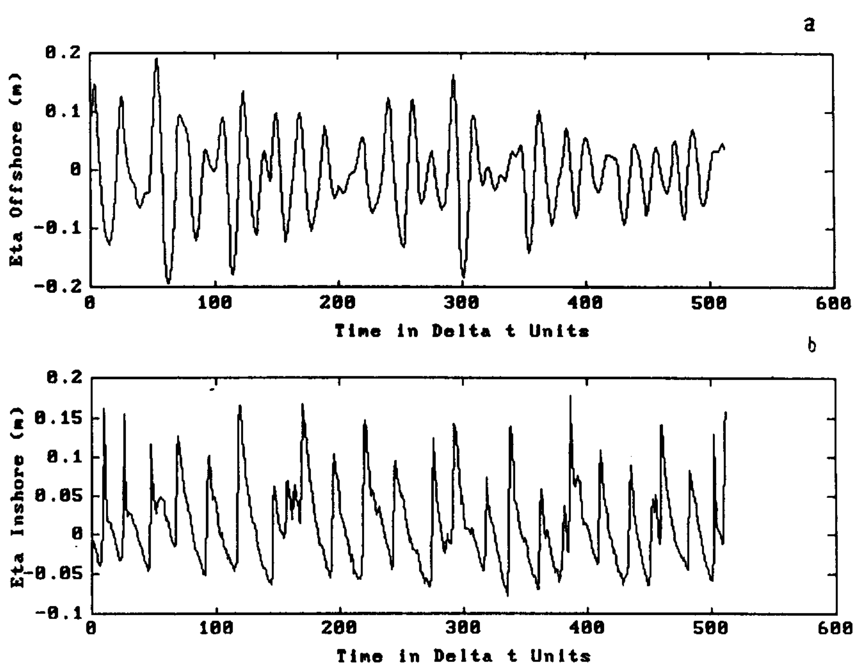

Fig. 31. Time series (a) offshore gage and (b) inshore gage wt2.

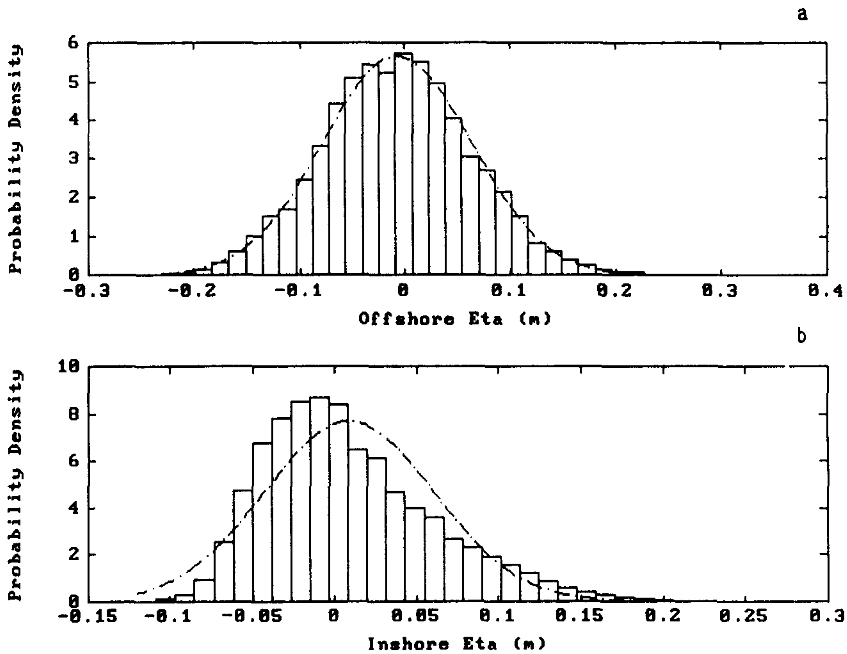

Fig. 32. Probability density (a) offshore and (b) inshore wt2.

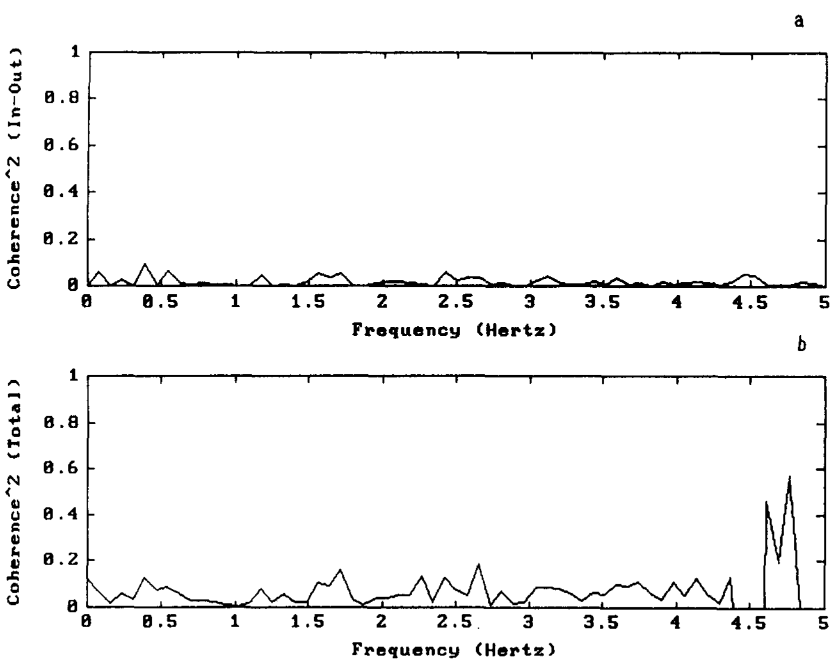

Fig. 33. Coherence wt2 (a) linear and (b) total (approach 1).

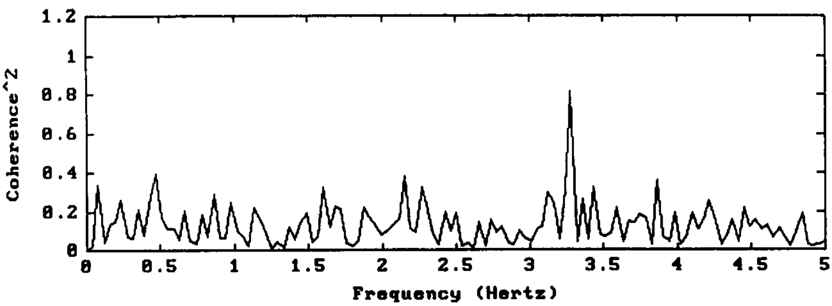

Fig. 34. Coherence wt2-total (approach 2).

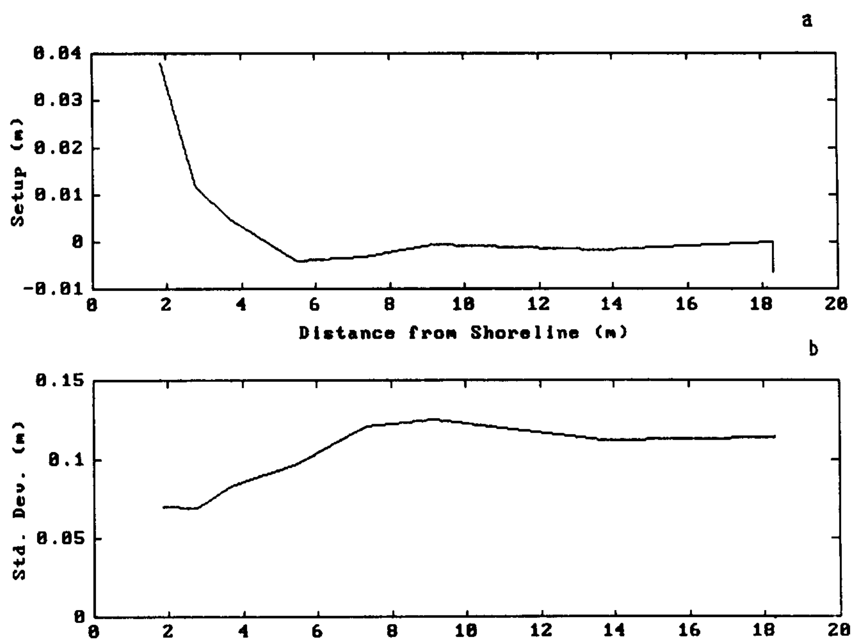

Fig. 35. (a) Setup and (b) variance of wt1.

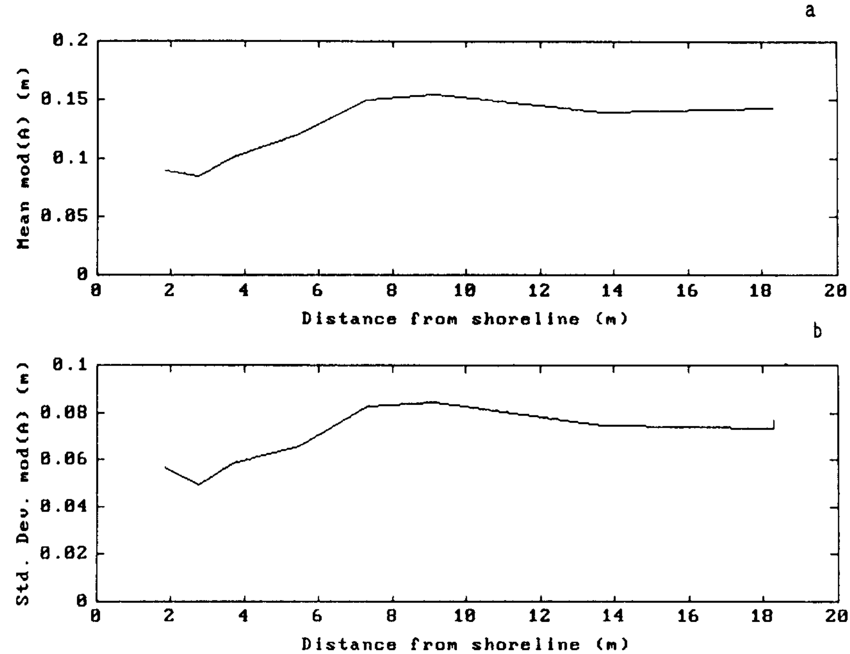

Fig. 36. (a) Mean and (b) std. dev. of envelope amplitude wt1.

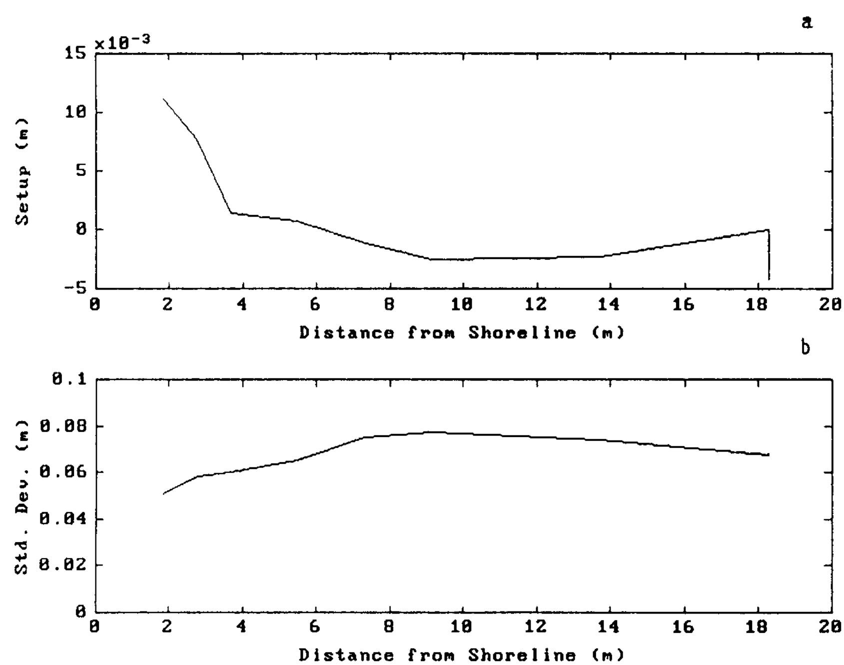

Fig. 37. (a) Setup and (b) variance of wt2.

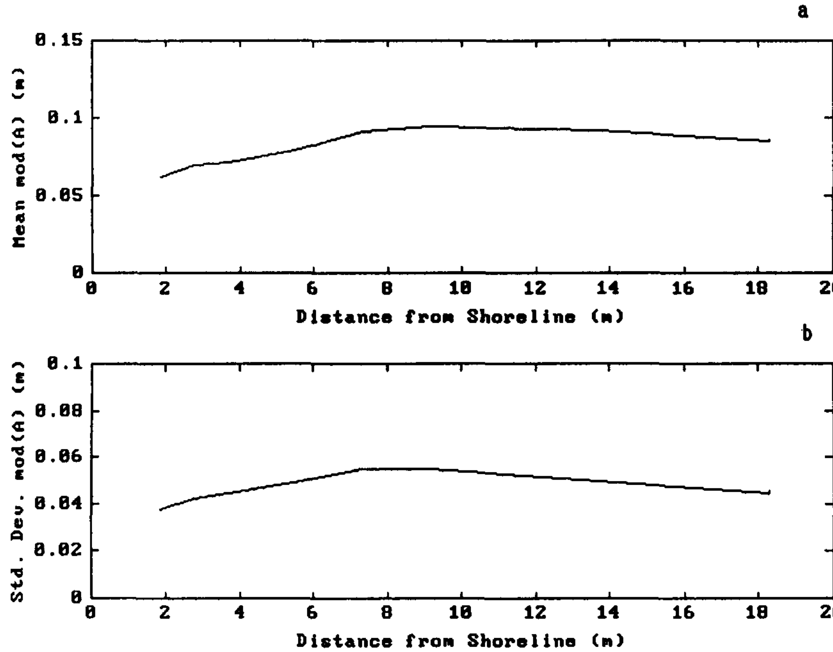

Fig. 38. (a) Mean and (b) std. dev. of envelope amplitude wt2.

breaking wave process. Further research on other possible approaches to this system identification problem should be attempted.

Acknowledgements—The work presented herein was conducted under the Irregular Wave Runup Work Unit of the Shore Protection and Restoration Research Program, United States Army Corps of Engineers, Coastal Engineering Research Center, U.S.A.E. Waterways Experiment Station. Permission was granted by the Office of Chief of Engineers, U.S. Army Corps of Engineers, to publish this information. The author would also like to thank Ms Jane Smith who provided the subset of wave tank data that was analyzed herein.

REFERENCES

Battjes, J.A. and Janssen, J.P.F.M. 1978. Energy loss and set-up due to breaking of random waves. In *Proc. 16th Conference Coastal Engineering, ASCE* **1**, 569–587.

Bendat, J.S. and Piersol, A.G. 1986. *Random Data: Analysis and Measurement Procedures*. (2nd Edition) John Wiley, New York.

Bendat, J.S. 1990. *Nonlinear System Analysis and Identification from Random Data*. John Wiley and Sons, New York.

Bendat, J.S. and Piersol, A.G. 1986. Decompositions of wave forces into linear and nonlinear components, *J. Sound Vibration* **81**, 199.

Bouws, E., Gunther, H., Rosenthal, W. and Vincent, C.L. 1985. Similarity of the wind wave spectrum in finite depth water, part I—spectral form. *J. Geophysical Res.* **90**, No. C1, 975–986.

Dally, W.R., Dean, R.G. and Dalrymple, R.A. 1985. Wave height variation across beaches of arbitrary profile. *J. Geophysical Res.* **90**, No. C6, 11,917–11,927.

Ebersole, B.A. and Hughes, S.A. 1987. Duck 85 photopole experiment. Coastal Engineering Research Center Miscellaneous Paper CERC-87-18, U.S.A.E. Waterways Experiment Station, Vicksburg, MS.

Elgar, S., Guza, R.T. and Seymour, R.J. 1984. Groups of waves in shallow water. *J. Geophysical Res.* **89**, No. C3, 3623–3634.

Elgar, S., Guza, R.T. and Seymour, R.J. 1985. Wave group statistics from numerical simulations of a random sea. *Appl. Ocean Res.* **7**, 93–96.

Goda, Y. 1975. Irregular wave deformation in the surf zone. *Coastal Engng Japan* **18**, 13–26.

Guza, R.T. and Thornton, E.B. 1982. Swash oscillations on a natural beach. *J. Geophysical Res.* **87**, 483–491.

Guza, R.T., Thronton, E.B. and Holman, R.A. 1984. Swash on steep and shallow beaches. In *Proc. 19th Int. Coastal Engineering Conf., ASCE,* New York, 708–723.

Holman, R.A. and Sallenger, A.H. Jr 1985. Set-up and swash on a natural beach. *J. Geophysical Res.* **90**, 945–953.

Horikawa, K. and Kuo, C.T. 1966. A study of wave transformation inside surf zone. *Proc. 10th Conference Coastal Engineering, ASCE* Vol. 1, 217–233.

Hotta, S. and Mizuguchi, M. 1980. A field study of waves in the surf zone. *Coastal Engng Japan, JSCE* **23**, 79–89.

Rye, H. 1982. Ocean wave groups. Report UR-82-18, Dept. Marine Technology, Norwegian Institute of Technology, Trondheim, Norway.

Smith, J.M. and Vincent, C.L. 1992. Shoaling and decay of two wave trains on a beach. Submitted for publication to ASCE Journal of Waterway, Port, Coastal, and Ocean Engineering.

Tribolet, J.M. 1977. A new phase unwrapping algorithm. In *IEEE Transactions on ASSP*, ASSP-25, **April**, pp. 170–177.

Walton, T.L. Jr. 1991. Investigation of two wave trains. (Unpublished File Report), U.S.A.E. Waterways Experiment Station, Coastal Engineering Research Center, Vicksburg, MS. 39180.

Walton, T.L. Jr. 1992. Wave reflection from natural beaches. *Ocean Engng* **19**, 239–258.